Available online www.jsaer.com

***Journal of Scientific and Engineering Research*, 2020, 7(3):229-237**

Research Article

ISSN: 2394-2630
CODEN(USA): JSERBR

Petrography and Mineral Chemistry of Mafic Metavolcanics of Baghmara Formation (Sonakhan Group), Raipur District, Chhattisgarh

S. D. Deshmukh[1]*, K. R. Hari[2], P. Diwan[3]

[1]Dept. of Geology, Govt.V.Y.T.P,G, Autonomous College, Durg, (C.G.)
deshmukhgeol@gmail.com
[2]S.O.S.in Geology and WRM, Pt. Ravishankar University, Raipur, India
[3]Dept. of Applied Geology, National Institute of Technology, Raipur (C.G.)

Abstract The Sonakhan Greenstone Belt (SGB) is a late Archaean Greenstone Belt covering an area of about 1200 Sq. km. along the north-eastern part of Raipur district of Chhattisgarh state. It comprises metavolcanic and metasedimentary sequences which have undergone greenschist to amphibolite facies of metamorphism. The supracrustals around Sonakhan and adjoining area are classified into relatively older Baghmara Formation dominated by mafic metavolcanics and felsic metavolcanics and a younger Arjuni Formation dominated by sandstone and polymictic conglomerate, the later includes clasts derived from Baghmara Formation. The two formations together constitute the Sonakhan Group.

The present paper presents an account of the petrography and mineral chemistry of Baghmara Formation. Petrographaic studies indicate that Baghmara Formation is a suite of bimodal metavolcanics. The pillow lavas of Baghmara Formation display characteristic features of metabasalts exhibiting low grade metamorphism (greenschist facies) represented by the mineral assemblage chlorite, actinolite and plagioclase minerals. The mineral chemistry of this assemblage has been studied by microprobe analysis. The presence of spinifex texture in these has been reported from the Sonakhan Greenstone Belt. The presence of spinifex texture suggests a komatiitic affinity for these metabasalts.

Keywords Sonakhan Greenstone Belt, petrography, mineral chemistry

1. Introduction

The Sonakhan Greenstone Belt, covering an area of about 1200 sq. km in north-eastern part of Raipur District, falls in S.O.I. toposheet Nos.64K/10 and 64K/11. It is bounded by 81^0 37' and 82^0 45' East longitudes and 21^0 17' and 21^0 37' North latitudes. It is situated at about 173 km. NE of Durg. One can approach the study area via Pithora which is located at about 100 km. from Raipur on NH-6. The study area includes Baghmara, Rajadeori, Sonakhan, Devgaon, Devpur, Nawagaon, Jungle Pahar, Amarua, Golajhar, Thelkadabri localities which are within a range of 35 to 45 km. to the North of Pithora.

The Sonakhan Greenstone Belt represents a late Archaean volcanosedimentary sequence which includes mafic and felsic metavolcanics with Banded Iron Formation and chert (Baghmara Formation) and the sedimentary sequence of conglomerate, greywacke, argillite along with B.I.F. and ferruginous chert (Arjuni Formation). The metavolcanics of Baghmara Formation have undergone greenschist to amphibolite facies of metamorphism. The Sonakhan Group rests unconformably over Baya Gneissic Complex. Structurally, it is a broad synformal basin with moderate plunge to the North- Northwest and closure to the South near Baya .

The Baghmara Formation forms the most prominent metavolcanic component of the Sonakhan Greenstone Belt and exhibits spectacular pillow structure formed by submarine emplacement of basaltic lavas**.** The level of

understanding of the geology of the study area is limited in comparison with most of the other Archaean and Proterozoic terrains.

The intensive study of greenstone belts and the question of their tectonomagmatic evolution remains one of the focal themes of Precambrian research. Furthermore, a number of large and largest, syn- or epigenetically formed nickel and gold ore deposits are confined to the greenstone belts. They owe their origin to the magmatic rocks and, therefore, to the processes of the evolution of magmas. This underlines the importance of the study of the processes of generation, transport and crystallization of the magmas during evolution of the greenstone belts.

2. Review of previous work

King [1] attempted to correlate Sonakhan beds with the Precambrians of Central India, namely Chilpighat and Sakoli series, whereas Pascoe [2] correlated the belt with the Dharwars of South India. Das *et al* [3] described the distribution of main lithological components of the belt and presented an updated stratigraphic succession of the area Saha et al [4] studied the structural relationship between the Baya Gneissic Complex and the Sonakhan Group. Venkatesh [5] carried out the ore mineralogical studies and suggested mesothermal origin for the gold mineralization in the area. Ray [6] mainly focussed their attention on the geochemistry and potentials of gold mineralization. Deshmukh et al [7] reported spinifex texture from mafic metavolcanics of Baghmara Formation of Sonakhan Greenstone Belt and deduced a komatiitic affinity for these rocks.

3. Material And Methods

Single disc grinding and polishing machine available in the Department of Applied Geology, N.I.T., Raipur, was used for the preparation of thin sections of various rocks for their microscopic studies. Rock names are based on field criteria. Although in some circumstances purely chemical definitions may be more appropriate, field definitions are generally adequate and provide continuity.

The electron microprobe analyses were carried out at EPMA Laboratory, Mineral Processing Division, Indian Bureau of Mines, Nagpur. All the thin sections were carbon coated prior to study by CAMECA-SX100 EPMA by wave-length dispersive spectrometry. A beam current of 12nA and an acceleration voltage of 15 kV were used along with a beam diameter of 1 micron.

Detailed megascopic and microscopic examination of the rocks was carried out for their petrographic characterization and to congregate evidences for possible petrogenetic processes undergone by them.

4. Petrography of Mafic Metavolcanics of Baghmara Formation

The mafic metavolcanics are represented by pillowed to massive/schistose metabasalts. Plagioclase, relict phases of clinopyroxene and opaque minerals (ilmenite and magnetite) form the primary mineral constituents with subordinate glassy material present in varying quantities. Summary of petrographic characters of mafic metavolcanics of Baghmara Formation is given in Table 1.

In metabasalt, the overall abundance of plagioclase phenocrysts in the thin sections ranges from 5% to 15%. The other phenocryst phases include clinopyroxene, magnetite, amphibole. The groundmass contains the same phases as are present as phenocrysts and also apatite. The probe analyses of apatite grains are given in Table 2. Secondary phases in some of the samples include chlorite, epidote, magnetite, ilmenite, and calcite. Breakdown to secondary chlorite or epidote was seen in clinopyroxene and plagioclase phenocrysts and the groundmass. Epidote occurs sporadically and is seen as green to light bluish pleochroic grains with high order interference colours (Fig. 1). The probe analyses of epidote reveal that the total FeO content varies from 9% to 14% (Table 3 and 4) indicating its Fe-rich nature.

The mineral assemblage exhibited by metabasalts is:

Plagioclase + actinolite+ chlorite+ opaques ± clinopyroxene ± epidote. ± apatite

Table 1: Summary of petrographic characters of mafic metavolcanics of Baghmara Formation

Sample No.	Rock Type	CPx.	Plagio clase	Chlorite	Opaque minerals	Actinolite	Epidote	Glass	Alteration	Noteworthy Texture
SK-1	Meta-basalt	XXX	XX	XX	X	XX	X	X	Chloritization	Intergranular
SK-2	Meta-basalt	XX	XX	XX	X	XX	X	X	Uralitization	Spinifex
SK-3	Meta-basalt	XXX	XX	XX	X	XX	XX	X	Uralitization	Spinifex
SK-4	Meta-basalt	X	XXX	XXX	X	XX	X	XX	Sausseritization	Pillotaxitic
SK-5	Meta-basalt	XXX	XX	X	X	XX	X	X	Albitization	Spinifex
SK-6	Meta-basalt	XXX	XX	X	XX	X	X	XX	Sausseritization	Intergranular
SK-7	Meta-basalt	XX	XX	XXX	X	X	XX	XX	Chloritization	Intergranular
SK-8	Meta-basalt	XX	XX	X	X	X	X	XXX	Albitization	Intersertal
SK-9	Meta-basalt	X	XXX	XXX	X	XX	X	XX	Albitization	Pillotaxitic
SK-10	Meta-basalt	X	XXX	XXX	X	XX	X	XX	Chloritization	Pillotaxitic
SK-11	Meta-basalt	XXX	XX	XX	X	XX	X	X	Chloritization	Intergranular
SK-12	Meta-basalt	X	XXX	XXX	X	XX	X	XX	Albitization	Pillotaxitic
SK-13	Meta-basalt	XXX	XX	X	XX	X	X	XX	Chloritization	Intergranular
SK-14	Meta-basalt	X	XXX	XXX	X	XX	X	XX	Chloritization	Pillotaxitic
SK-15	Meta-basalt	XX	XXX	XX	X	X	X	XX	Sausseritization	Intersertal
SK-16	Meta-basalt	XXX	XX	XX	X	XX	X	X	Chloritization	Intergranular
SK-17	Meta-basalt	XXX	XX	XX	X	X	X	X	Uralitization	Spinifex
SK-18	Meta-basalt	XXX	XX	XX	X	XX	XX	X	Uralitization	Spinifex
SK-19	Meta-basalt	XX	XXX	XXX	X	X	X	XX	Sausseritization	Pillotaxitic
SK-20	Meta-basalt	XXX	XX	X	X	XX	XX	X	Albitization	Spinifex
SK-51	Meta-basalt	XX	XXX	XXX	X	XX	X	XX	Sausseritization	Pillotaxitic

Table 2: Probe analyses of apatite grains

Oxide	1	2	3	4
Na_2O	0.12	0.03	0.03	0.05
MgO	0.04	0	0	0.03
Al_2O_3	0.01	0	0	0
SiO_2	1.59	0	1.04	0
P_2O_5	42.79	43.36	44.12	43.86
K_2O	0	0	0.08	0.01
CaO	54.19	56.29	56.28	56.82
TiO_2	0.12	0	0	0
Cr_2O_3	0	0	0	0
MnO	0.08	0.01	0.06	0.01
FeO	0.49	0.03	0.45	0.15
Total	99.44	99.72	102.06	100.92

Table 3: Probe analyses of epidote grains

Oxide	1	2	3	4	5	6	7	8
SiO_2	35.74	35.88	36.44	35.85	35.73	37.12	37.58	32.7
TiO_2	0.04	0.09	0.01	0	0.06	0	0.07	0.06
Al_2O_3	24.15	25.59	22.94	23.81	22.38	23.42	23.68	22.51
Cr_2O_3	0.02	0.05	0	0.01	0	0.05	0	0.02
FeO	11.97	9.11	12.99	12.47	12.98	12.2	12.12	13.8
MnO	0.18	0.2	0.07	0.06	0.11	0.14	0.11	0.03
MgO	0.03	0.02	0.08	0.04	0.03	0	0.04	0
CaO	23.42	23.43	23.5	23.5	23.56	23.27	23.6	23.65
Na_2O	0	0	0.39	0.31	0	0.02	0.01	0
K_2O	0	0	0.03	0	0	0.03	0	0
Totals	95.55	94.37	96.45	96.05	94.85	96.25	97.21	92.77

Table 4: Cations per formula unit of epidote (calculated on the basis of 12.5 'O')

Cation	1	2	3	4	5	6	7	8
Si	2.986831	2.987384	3.03500812	2.990738	3.030741	3.072659	3.075747	2.873901
Ti	0.002514	0.0056356	0.00062638	0	0.003828	0	0.004309	0.003966
Al	2.379364	2.5118661	2.25248793	2.341726	2.238018	2.285498	2.284879	2.332314
Cr	0.001321	0.0032911	0	0.00066	0	0.003272	0	0.00139
Fe	0.836615	0.6343551	0.90482808	0.870024	0.920801	0.844582	0.829606	1.014328
Mn	0.012742	0.0141052	0.00493845	0.00424	0.007904	0.009816	0.007626	0.002233
Mg	0.003736	0.0024817	0.00993009	0.004973	0.003792	0	0.004879	0
Ca	2.097187	2.0902831	2.09721787	2.100638	2.141339	2.06394	2.069665	2.227149
Na	0	0	0.06298146	0.050144	0	0.00321	0.001587	0
K	0	0	0.00318775	0	0	0.003168	0	0
Totals	8.320312	8.2494018	8.37120614	8.363142	8.346422	8.286145	8.278298	8.455282

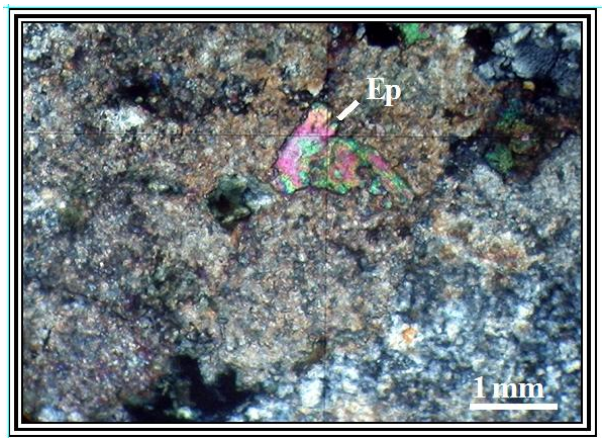

Figure 1: Photomicrograph showing Epidote (Ep) in metabasalt (under XPL)

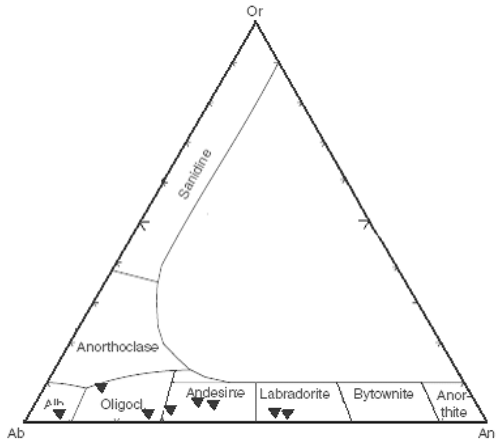

Figure 2 : Composition of plagioclase grains on the basis of probe analyses

Plagioclase occurs both as phenocrysts and as a constituent of groundmass. Prismatic plagioclase phenocrysts show variation in composition ranging from labrodorite to albite (Fig. 2). As a constituent of groundmass the plagioclase grains are microcrystalline (Fig. 3). Acicular plagioclase grains give rise to immature sheaf quenched texture in a few thin sections. Triangular network of plagioclase laths with pyroxene and glassy material occupying the interstices was also observed thus exhibiting intergranular and intersertal textures (Fig. 4) and at places it grades into hyalopilitic texture. In a few cases the small plagioclase laths show random orientation giving rise to pillotaxitic texture. In some cases the plagioclase laths and other mineral constituents show parallel orientation along their length in the thin section (Fig. 5). Plagioclase is commonly seen altered into clay minerals and at places into clinozoisite (Fig. 6). Albitization is prominently seen in the thin sections and has been confirmed as Ab_{76}- Ab_{92} from the probe analyses (Table 5 and 5a).

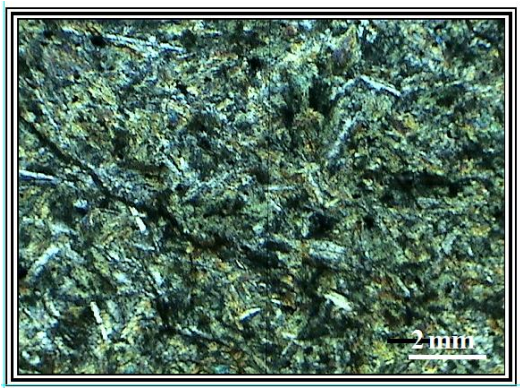

Figure 3: Photomicrograph showing microcrystalline plagioclase grains in metabasalt (under XPL)

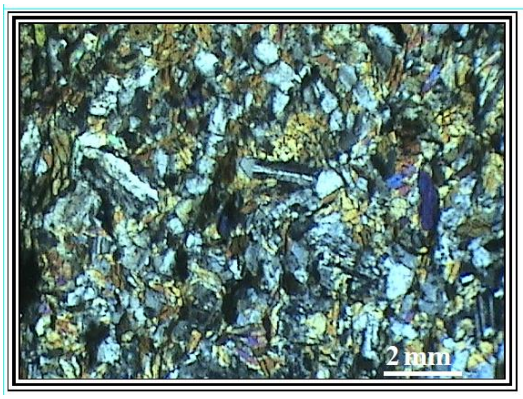

Figure 4: Photomicrograph exhibiting intergranular texture in metabasalt (under XPL)

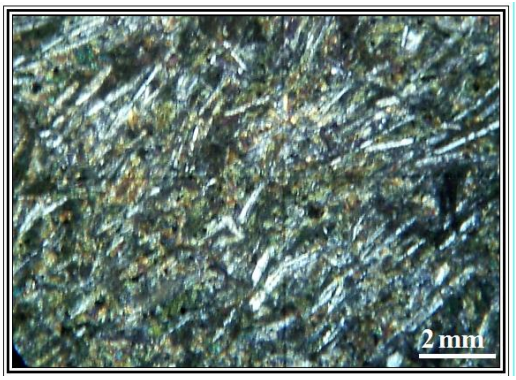

Figure 5: Photomicrograph exhibiting subparallel arrangement of plagioclase laths in metabasalt (under XPL)

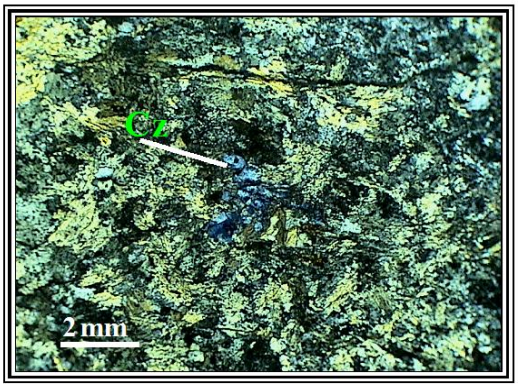

Figure 6: Photomicrograph showing clinozoisite (Cz) in metabasalt (under XPL)

Relict phases of clinopyroxene are seen in various thin sections; they occur both as phenocrysts and as a common constituent of the groundmass (Fig. 7 & 8). Clinopyroxene exhibits quench crystal morphologies intergrown with plagioclase sheafs at many places giving rise to spinifex texture indicating a komatiitic affinity for these rocks (Figs.9 & 10). In some portions the phenocrysts of clinopyroxene are seen altered into chlorite to various degrees (Fig. 11). Deformation and bending of clinopyroxene altered to actinolite was also observed and opaque minerals partly occupied the cracks along cleavages (Fig. 12). Probe analyses of the sections show that the pyroxenes are of the augite to ferroaugite composition (Fig. 13 and Table 6).

Table 5: Probe analysis of plagioclase grains

Oxide	1	2	3	4	5	6	7	8
SiO_2	55.49	68.81	54.19	78.81	58.68	54.58	65.42	61.77
TiO_2	0.00	0.07	0.00	0.47	0.11	0.00	0.04	0.00
Al_2O_3	28.81	17.66	28.39	9.86	24.56	24.79	20.69	23.56
Cr_2O_3	0.05	0.00	0.02	0.00	0.04	0.03	0.01	0.00
FeO	1.11	0.19	1.16	0.47	1.00	0.84	0.07	0.37
MnO	0.00	0.00	0.01	0.00	0.00	0.00	0.00	0.00
MgO	0.12	0.04	0.12	0.18	0.31	0.14	0.00	0.00
CaO	11.81	1.41	12.09	2.80	1.68	5.59	2.73	4.97
Na_2O	4.81	9.48	5.07	5.01	7.29	7.64	10.73	8.94
K_2O	0.00	0.04	0.03	0.06	3.11	1.22	0.04	0.13
Total	102.2	97.70	101.08	97.66	96.78	94.83	99.73	99.74

Table 5(a): Cations per formula unit of plagioclase grains

Cation	1	2	3	4	5	6	7	8
Si	1.845448	2.294934	1.830179	2.5654271	2.03332961	1.947895	2.169676	2.063721
Ti	0	0.001756	0	0.0115062	0.00286659	0.0	0.000998	0
Al	1.129582	0.69438	1.130388	0.3783928	1.00330647	1.043028	0.80897	0.927975
Cr	0.001315	0	0.000534	0	0.00109574	0.000846	0.000262	0
Fe	0.030873	0.0053	0.032765	0.0127953	0.02897965	0.025072	0.001942	0.010338
Mn	0	0	0.000286	0	0	0	0	0
Mg	0.005948	0.001988	0.00604	0.0087324	0.01600888	0.007446	0	0
Ca	0.420854	0.050389	0.437517	0.0976631	0.06237652	0.213766	0.097016	0.17792
Na	0.310169	0.613047	0.332008	0.3162152	0.48979215	0.528679	0.690002	0.579132
K	0	0.001702	0.001293	0.0024918	0.13748628	0.055549	0.001692	0.005541
Total	3.744189	3.663495	3.77101	3.3932238	3.77524191	3.822281	3.770558	3.764628
Ab%	42.42948	92.16845	43.07221	75.9457	71.0198843	66.25105	87.48489	75.94249
Or%	0	0.255887	0.167697	0.5984549	19.9355171	6.961037	0.214589	0.726617
An%	57.57052	7.575663	56.76009	23.455845	9.04459863	26.78791	12.30052	23.33089

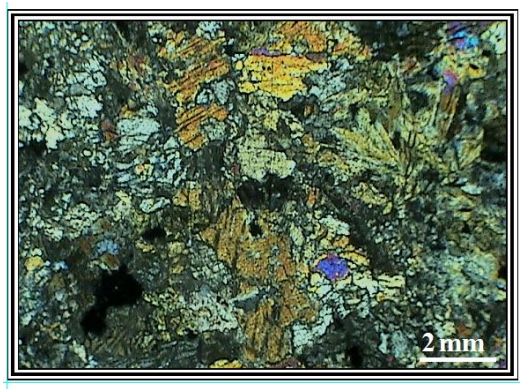

Figure 7: Photomicrograph showing clinopyroxene in metabasalt (under XPL)

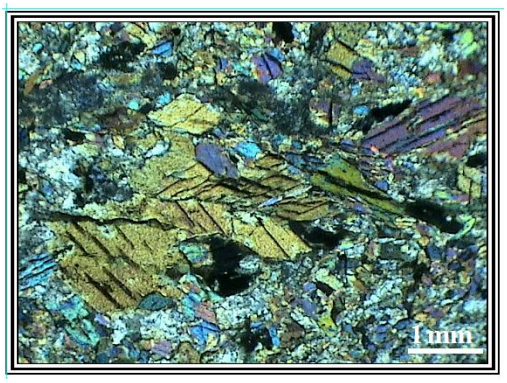

Figure 8: Photomicrograph showing clinopyroxene in metabasalt (under XPL)

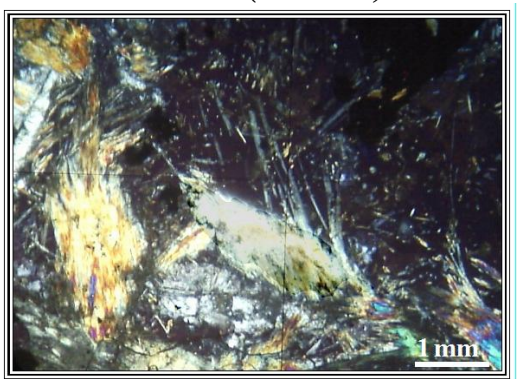

Figure 9: Photomicrograph showing spinifex texture in metabasalt (under XPL)

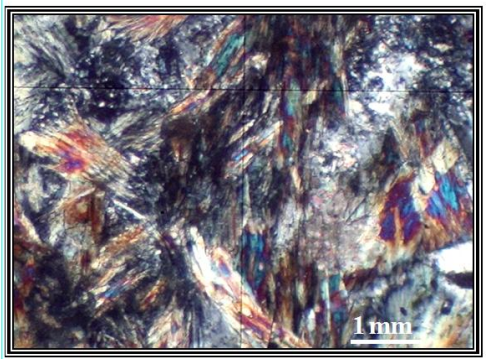

Figure 10: Photomicrograph showing spinifex texture in metabasalt (under XPL)

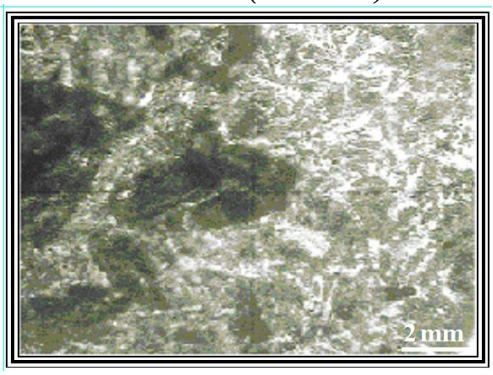

Figure 11: Photomicrograph showing chloritization in meta-basalt (under PPL)

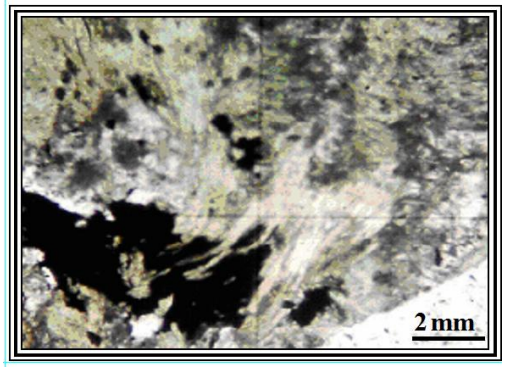

Figure 12: Photomicrograph showing deformation in altered clinopyroxene in meta-basalt (under PPL)

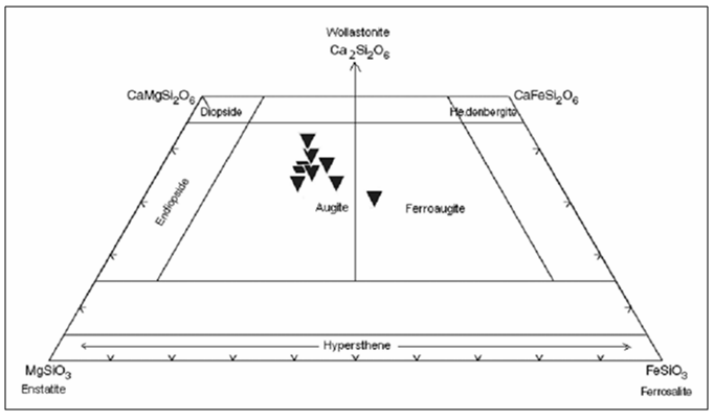

Figure 13: composition of the pyroxene grains as depicted by probe analysis

Table 6: Probe analyses of the pyroxene grains

Oxide	1	2	3	4	5	6	7	8	9
SiO_2	47.95	46.09	46.9	45.07	46.86	48.66	46.23	44.1	44.84
TiO_2	0.11	0.27	0.14	0	0.05	0.06	0.63	0	0.62
Al_2O_3	5.25	4.49	4.05	4.78	4.11	4.51	2.48	4.3	2.26
Cr_2O_3	0.16	0	0.02	0	0.01	0	0.04	0	0.02
FeO	17.75	16.56	16.29	16.46	15.88	15.77	13.69	21.61	15.06
MnO	0.23	0.28	0.22	0.19	0.29	0.23	0.22	0.21	0.43
MgO	11.88	13.25	13.01	13.93	13.87	13.26	13.73	10.75	14.57
CaO	12.47	12.34	12.58	11.66	12.19	12.8	17.8	11.48	17.27
Na_2O	0.6	0.39	0.4	0.31	0.32	0.33	0.25	0.42	0.25
K_2O	0.07	0.05	0.07	0.05	0.02	0.04	0.01	0.21	0.03
Totals	96.47	93.72	93.68	92.45	93.6	95.66	95.08	93.08	95.35

Cation	1	2	3	4	5	6	7	8	9
Si	1.889383	1.868613	1.897409	1.850845	1.891332	1.91334	1.858368	1.851411	1.816946
Ti	0.00326	0.008233	0.00426	0	0.001518	0.001774	0.019046	0	0.018894
Al	0.243881	0.214608	0.193166	0.231418	0.195567	0.209066	0.11753	0.212824	0.107962
Cr	0.004984	0	0.00064	0	0.000319	0	0.001271	0	0.000641
Fe	0.584932	0.561498	0.551169	0.565311	0.536033	0.518594	0.460242	0.758743	0.51036
Mn	0.007677	0.009616	0.007539	0.006609	0.009915	0.007661	0.007491	0.007468	0.014759
Mg	0.697637	0.80059	0.784417	0.852541	0.834303	0.777043	0.822546	0.672596	0.879868
Ca	0.526492	0.536071	0.545334	0.513068	0.527185	0.539292	0.766694	0.516417	0.74983
Na	0.04584	0.030658	0.031377	0.024684	0.025043	0.025159	0.019486	0.034189	0.019642
K	0.003519	0.002586	0.003613	0.00262	0.00103	0.002007	0.000513	0.011248	0.001551
Totals	4.007605	4.032473	4.018924	4.047097	4.022244	3.993936	4.073185	4.064895	4.120454
Mg%	0.385635	0.421772	0.417039	0.44152	0.43968	0.423473	0.401343	0.345319	0.411142
Ca%	0.291031	0.282416	0.28993	0.265712	0.277829	0.293904	0.374092	0.265134	0.350378
Fe%	0.323334	0.295812	0.293031	0.292768	0.282491	0.282623	0.224565	0.389547	0.23848

Table 7: Probe analyses of the amphibole grains

Oxide	1	2	3	4
SiO_2	58.91	57.42	51.63	53.54
TiO_2	0.99	0.36	0.26	0.12
Al_2O_3	1.3	1.38	2.24	0.84
Cr_2O_3	0	0.01	0	0.1
FeO	14.81	15.76	19.19	20.81
MnO	0.29	0.2	0.26	0.27
MgO	9.08	9.81	11.23	8.92
CaO	13.15	10.84	12.66	11.21
Na_2O	0.1	0.11	0.27	0.18
K_2O	0.07	0.01	0.08	0.02
Totals	98.7	95.9	97.82	96.01

Cation	1	2	3	4
Si	8.727209	8.747944	8.020401	8.454256
Ti	0.1103	0.041248	0.030375	0.014251
Al	0.227048	0.247862	0.410232	0.156374
Cr	0	0.001204	0	0.012483
Fe	1.834919	2.00805	2.493127	2.748176
Mn	0.036391	0.02581	0.034212	0.036114
Mg	2.004721	2.227376	2.599892	2.09915
Ca	2.087403	1.769564	2.107278	1.896692
Na	0.028725	0.032494	0.081325	0.055111
K	0.01323	0.001944	0.015855	0.004029
Totals	15.06995	15.10349	15.7927	15.47664

Table 8: Probe analyses of the chlorite grains

Oxide	1	2	3	4	5
SiO_2	22.47	24.89	22.77	29.14	27.67
TiO_2	0	0.06	0.26	0.08	0.02
Al_2O_3	18.81	19.71	19.08	20.15	19.48
Cr_2O_3	0.08	0.03	0.14	0.04	0.01
FeO	24.84	33.24	31.79	29.97	26.8
MnO	0.35	0.41	0.44	0.36	0.5
MgO	17.1	10.23	10.27	8.83	13.59
CaO	0.14	0.08	0.14	0.15	0.17
Na_2O	0	0.05	0.05	0.44	0.05
K_2O	0	0.01	0	0.19	0
Totals	83.79	88.71	84.94	89.35	88.29

Cation	1	2	3	4	5
Si	5.033129	5.432201	5.2130112	6.12007663	5.818636
Ti	0	0.009848	0.0447666	0.01263609	0.003163
Al	4.967197	5.071368	5.1498143	4.98918874	4.829349
Cr	0.014166	0.005176	0.0253387	0.00664139	0.001662
Fe	4.65331	6.067187	6.0868358	5.26416492	4.71327
Mn	0.066407	0.075796	0.0853276	0.06404435	0.089062
Mg	5.708379	3.327425	3.5041101	2.76381963	4.259054
Ca	0.033601	0.018708	0.0343438	0.03375614	0.038305
Na	0	0.021159	0.0221954	0.17917879	0.020387
K	0	0.002784	0	0.0509099	0
Total	20.47619	20.03165	20.165743	19.4844166	19.77289

Uralitization of clinopyroxene and development of secondary amphibole (commonly actinolite) was prominently seen in majority of thin sections. The actinolite grains are elongate prismatic to acicular aggregates the probe analysis of amphibole grains is as given in Table 7 and show greenish blue to light green pleochroic colours. Radiating aggregates of feathery pyroxene and actinolite have also been observed displaying partly developed variolitic texture in the thin section (Fig. 14). Most of the thin sections show varying degrees of chloritization. Chlorite forms significant part of groundmass in many sections. It shows iron enrichment, as deduced by the dark green colour and confirmed by the probe analyses (Table 8).

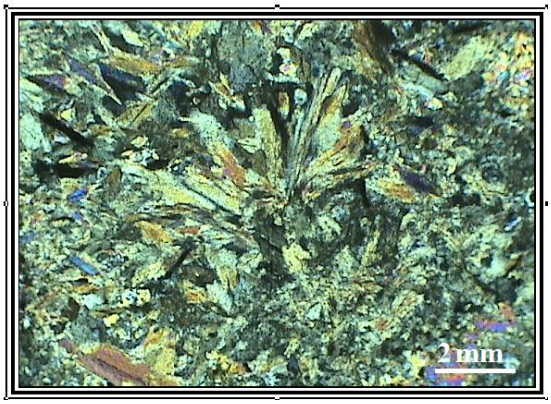

Figure 14: Variolitic texture in metabasalt(under XPL)

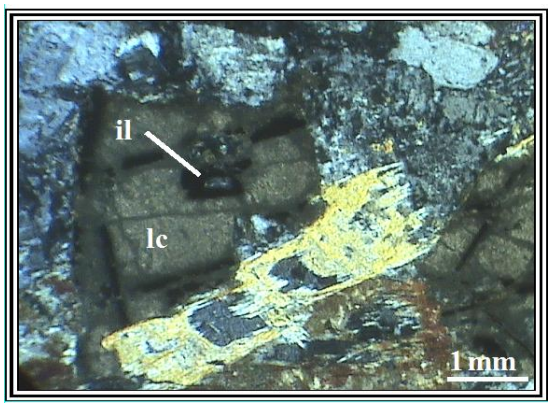

Figure 15: Alteration of ilmenite (il) into leucoxene (lc) in metabasalt (under XPL) (under XPL)

Opaque minerals (ilmenite, rutile and magnetite) are common in the metabasalts. Fine grains are seen dispersed throughout few thin sections imparting a salt and pepper appearance. The probe analyses of the opaque minerals are given in the (Table 9). Ilmenite is seen as laths and also as coarse irregular grains. The coarse grains, in many cases are seen altered to leucoxene (Fig.15) . The probe analyses show a variation of 55% to 64% TiO_2 and 32% to 41% FeO (Table 9). Magnetite is seen as subhedral grains and is commonly scattered in the groundmass. The FeO varies from 58% to 80%. In some of the cases the TiO_2 approached 10% imparting titanomagnetite nomenclature to some of the grains . Some rutile grains are also noticeable in the thin sections and the TiO_2 content varies from 85% to 96% .Glass, in varying quantities is commonly seen present in metabasalts occupying interstices among plagioclase, occupying interstices among plagioclase, pyroxene, actinolite and opaques. Glass also locally showed alteration into yellowish brown palagonite. The back scattered electron images of probe sections showing various mineral constituents observed during electron micro probe analyses are shown in Figs.16 & 17.

Table 9: Probe analyses of opaque minerals

Oxide	Rutile				Ilmenite			Magnetite					
	1	2	3	4	1	2	3	1	2	3	4	5	6
SiO_2	2.34	0	0.98	6.6	0	0	0	0	0	0	7	9.01	4.85
TiO_2	93.22	98.07	95.34	84.78	63.84	58.41	55.3	0.05	0	0.04	0.51	9.67	0.07
Al_2O_3	2.97	0.82	1.22	4.87	0.01	0	0.01	7.04	0	0.01	0.54	1.84	0.01
Cr_2O_3	0.05	0.07	0.06	0.02	0.05	0.08	0	0.09	0.06	0	0.12	0	1.31
FeO	0.34	0.24	1.09	1.02	32.58	37.95	41.1	76.59	79.71	57.7	78	64.62	87.6
MnO	0	0	0	0	0.28	0.25	0.2	0.11	0	0.02	0.06	0	0.03
MgO	0.07	0	0.04	0.12	0.05	0.02	0	0.27	0	0.05	1.93	0.66	0.02
CaO	0.02	0.02	0.03	0.02	0.46	0.26	0.15	1.06	0.07	0.09	2.53	6.75	0.21
Na_2O	0.15	0.01	0.1	0.19	0.05	0.01	0.1	0	0.02	0	0.41	0.03	0.04
K_2O	0.61	0.32	0.38	1.17	0.01	0	0	0.01	0	0	0.02	0.04	0.07
Total	99.77	99.55	99.26	98.79	97.31	96.97	96.87	88.18	79.85	57.91	91.12	92.61	94.21

Cation	Rutile				Ilmenite			Magnetite					
	1	2	3	4	1	2	3	1	2	3	4	5	6
Si	0.030962	0	0.01316	0.087221	0	0	0	0	0	0	2.570898	2.938053	1.825835
Ti	0.927648	0.986827	0.962861	0.842608	2.319271	2.192395	2.114774	0.015363	0	0.019839	0.140841	2.371465	0.019819
Al	0.04633	0.012935	0.019314	0.075874	0.000569	0	0.000599	3.390931	0	0.007775	0.233767	0.70736	0.004438
Cr	0.000523	0.00074	0.000637	0.000209	0.001909	0.003156	0	0.029069	0.022713	0	0.034835	0	0.389872
Fe	0.003762	0.002686	0.012242	0.011273	1.316224	1.58403	1.747836	26.17015	31.92073	31.82474	23.95368	17.62289	27.58032
Mn	0	0	0	0	0.011457	0.010569	0.008614	0.038068	0	0.011173	0.018662	0	0.009566
Mg	0.00138	0	0.000801	0.002363	0.0036	0.001488	0	0.164401	0	0.049143	1.056188	0.320745	0.011221
Ca	0.000284	0.000287	0.000432	0.000283	0.02381	0.013904	0.008173	0.464044	0.035915	0.063599	0.995444	2.358483	0.08471
Na	0.003848	0.000259	0.002604	0.004869	0.004683	0.000968	0.009859	0	0.018569	0	0.291913	0.018968	0.029198
K	0.010297	0.005462	0.00651	0.019726	0.000616	0	0	0.005212	0	0	0.009369	0.016641	0.03362
Total	1.025086	1.009196	1.01856	1.044427	3.682139	3.80651	3.889856	30.27724	31.99793	31.97627	29.3051	26.35461	29.9886

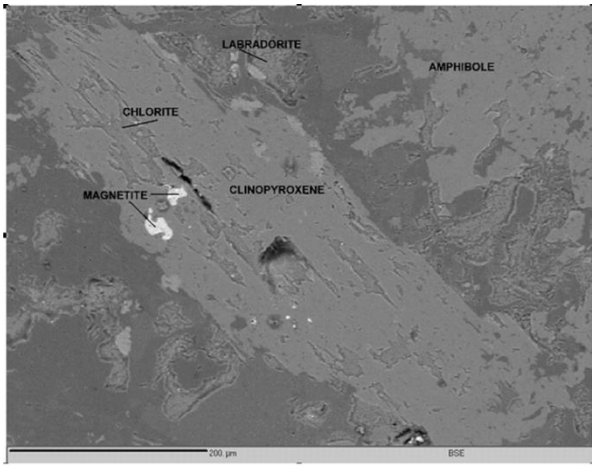

Figure 16 : BSE image of metabasalt (SK-5) exhibiting various mineral constituents

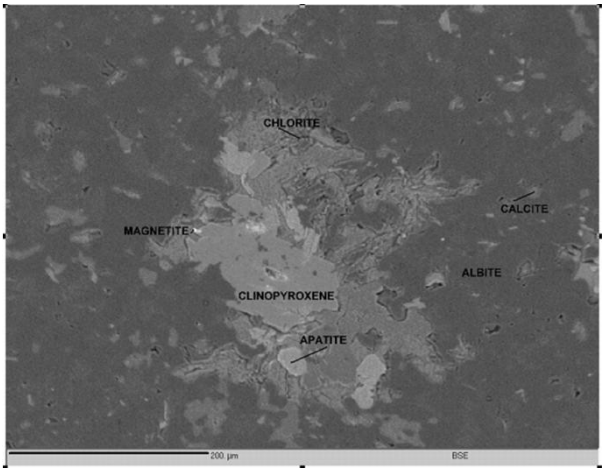

Figure 17 : BSE image of metabasalt (SK-9) exhibiting various mineral constituents

5. Discussion and conclusion

Petrographaic studies indicate that the pillow lavas of Baghmara Formation display characteristic features of metabasalts exhibiting low grade metamorphism (greenschist facies) represented by the mineral assemblage pyroxene + plagioclase+ chlorite + actinolite + opaques. The mineral chemistry of this assemblage has been studied by microprobe analysis. Petrographic studies revealed presence of spinifex texture, thus indicating a komatiitic affinity for the basalts. The other common textures observed are intergranular, intersertal, pillotaxitic, variolitic which are common in tholeiitic basalts. The study of petrography and mineral chemistry of mafic metavolcanics of Baghmara Formation resembles that of mafic metavolcanic components of well documented greenstone belts elsewhere in the world.

Acknowledgement

The authors are thankful to Dr. R. N. Singh, Principal, Govt. V.Y.T.P.G. Autonomous College, Durg, for his encouragement. The authors are also thankful to Dr. Sandeep Vansutre and Dr. Vikas Swarnkar for their help in the preparation of the manuscript. Financial assistance from UGC in the form of a minor research project to S.D. Deshmukh is gratefully acknowledged.

References

[1]. King W. (1899). General Report for 1889-1899 . Geol. Surv. India. pp. 39-42.
[2]. Pascoe E.H. (1950). A Manual of Geology of India and Burma . Vol . 1, Govt. of India Publication, New Delhi.
[3]. Das, N., Royburman, K.J., Vatsa, U.S. and Mahurkar, V.Y. (1990). Sonakhan Schist Belt -A Precambrian granite – greenstone complex. Geol. Surv. India Sp. Pub. No. 28 , pp. 118-132 .
[4]. Saha,D., Deb, G.K. and Dutta, S. (1998): Granite greenstone relationship in the Sonakhan Belt, Raipur District, Central India. Proceedings Volume. Int. Sem. Precambrian Crust in Eastern and Central India, IGCP-368, Bhubaneshwar.
[5]. Venkatesh A.S. (2001) Geochemical signatures and auriferous implications in Sonakhan Greenstone Belt, Chhattisgarh.Geol.Surv.India.Spl.Pub.No.55, pp. 219-228.
[6]. Ray, R.K. and Rai, K.L.(2004): Geological setting and petrogenesis of the auriferous metavolcanic complex of Sonakhan, Raipur district, Chhattisgarh. SAAEG Jour. of Eco. Geol. v.1. pp. 45-60.
[7]. Deshmukh S.D., Hari K.R., Diwan P., Basavarajappa H.T. (2008): Spinifex textured metabasalt from Sonakhan Greenstone Belt, CentralIndia. Indian Miner 42:71–83